Exchange frustration and transverse spin freezing in iron-rich metallic glasses

Hong Ren and D. H. Ryan
Centre for the Physics of Materials, Physics Department, Rutherford Building, McGill University, 3600 University Street, Montreal, Quebec, Canada H3A 2T8

(Received 15 June 1994; revised manuscript received 16 January 1995)

The magnetic properties of several iron-rich amorphous alloys of the form a-Fe_xT_{100-x} (T=Zr,Hf,Sc; $x\sim 90$) have been studied down to 5 K using magnetization measurements and Mössbauer spectroscopy, both with and without an external magnetic field. Two magnetic transitions are observed: first to a collinear magnetic state at T_c, then noncollinearity develops at T_{xy}. Analysis of the composition and temperature dependences of the magnetic ordering allows us to rule out cluster-based models of the behavior. All of our results can be explained in terms of a homogeneous freezing of transverse spin components at T_{xy} leading to a state in which ferromagnetic and spin-glass order coexist. Quantitative agreement with Monte Carlo simulations of a bond-frustrated Heisenberg system is observed.

I. INTRODUCTION

One approach to the study of spin glasses is to view ferromagnets and spin glasses as two extremes of a continuum. One may begin with a system having only ferromagnetic exchange, FM, (at $T=0$ for simplicity) and add antiferromagnetic exchange randomly to form $(FM)_{1-x}(AF)_x$. It is unlikely that an infinitesimal concentration would immediately destroy the long-ranged order, as all real materials contain some impurities and such a loss would preclude the experimental observation of ferromagnets. However, with equal amounts of FM and AF exchange present ($x=0.5$) the disorder and exchange frustration lead to a spin glass.[1-3] Thus at some concentration, $0<x\leq 0.5$, the long-ranged order must disappear. The phase transition between the paramagnetic (PM) and ordered states may also be lost. The evolution from FM to spin glass (SG) with increasing x allows one to study how the spin glass evolves out of the ferromagnet as a function of concentration (or equivalently, frustration). This approach complements the more conventional studies of fixed composition evolution from paramagnet to spin glass with temperature.

Partially frustrated systems are readily constructed, both experimentally and theoretically, and studies have revealed a rich pattern of ordering behavior.[4,5] Two magnetic ordering events are observed: the first (at T_c) marks the onset of long-range ferromagnetic order, while at the second, lower, transition (T_{xy}) transverse degrees of freedom freeze randomly without affecting the collinear (z) component of the order and thus the system retains a net ferromagnetic moment. At $T=0$ ferromagnetic and spin-glass order coexist. The freezing of transverse components causes the system to enter a noncollinear state and, although the xy components contribute to the total moment, they do not affect the magnetization; thus while the two parameters match above T_{xy}, below it, the total ordered moment is larger than the magnetization. Below T_{xy} the systems exhibit many of the characteristics of spin glasses—e.g., noncollinear order, strong magnetic irreversibility, and time-dependent magnetization—this has resulted in such materials being called "reentrant spin glasses" (RSG) by imperfect analogy with reentrant superconductors. However, they do not reenter the normal (in this case paramagnetic) state at T_{xy}, as there is no loss of collinear order down to $T=0$, even after the transverse spin components freeze.

Iron-rich amorphous alloys of the form Fe_xT_{100-x} where T is an early transition metal, e.g., Sc,[6,7] Y,[8,9] Zr,[10] or Hf,[11] are ideal systems for studying the effects of partial exchange frustration. They contain a single magnetic species, Fe, which avoids the problems of nonrandom substitution, a complication which has colored much of the discussion of ordering in RSG and led to descriptions in terms of isolated, finite clusters of spins somewhat reminiscent of the "mictomagnet" picture originally suggested as a description of spin glasses.[12] Iron is present at high concentrations (typically $\sim$90%), eliminating the possibility of percolation effects, and leading to relatively high transition temperatures. Exchange frustration arises through the distance dependence of the Fe-Fe direct exchange interaction, which changes sign at about 2.55 Å [closer contacts being AF, more distant ones being FM (Refs. 13 and 14)]. The large moments and strong exchange reflected in the high transition temperatures mean that exchange effects dominate the ordering. The alloys are prepared by melt spinnning, and the rapid quenching from the liquid state leads to extreme compositional uniformity, eliminating the possibility of chemical segregation. Finally, their magnetic properties span the full range of possibilities from ferromagnet, for T=Zr at $x=88$, to spin glass, for T=Sc at $x\sim 90$.[15]

The a-Fe_xZr_{100-x} system with $x>85$ is the most widely studied of the a-FeT glasses, and all of the features of RSG behavior have been observed. These include the drop of magnetic ordering temperature, T_c, with increasing Fe concentration without a corresponding decrease in the Fe moment,[10] irreversible dc susceptibility χ_{dc},[16] and two peaks in χ_{ac} in the presence of a small dc field.[17] Mössbauer spectra of a-$Fe_{93}Zr_7$ measured in a field applied parallel to the γ beam indicate that the system becomes noncollinear at a temperature T_{xy} well below

T_c.[18,19] It was also found that below T_{xy}, the average iron moment obtained from Mössbauer spectra is larger than that derived from magnetization.[18] These observations were explained in terms of transverse spin freezing,[4,10,18,20] which is similar to the mean-field model for Heisenberg spins developed by Gabay and Toulouse.[2] Furthermore, numerical simulations[3] accurately reproduce the experimental observations.

Experimental data on a-Fe-Hf is more limited.[21–23] However, applied field Mössbauer spectroscopy and high-field magnetization data[11] confirm that these alloys are not collinear ferromagnets, and it appears that a-Fe-Hf alloys exhibit similar behavior to a-Fe-Zr alloys, consistent with the strong chemical and physical similarities between Zr and Hf. By contrast, the magnetic behavior of a-Fe-Sc alloys seems quite different. Melt-spun a-$Fe_{90}Sc_{10}$ was first prepared and studied by Day *et al.*[6] A sharp cusp at 99 K in ac susceptibility (χ_{ac}) was observed, suggesting a spin-glass state at low temperatures. Ryan *et al.*[7] have shown that all of the samples they studied (a-Fe_xSc_{100-x}, $x=89-91$) exhibited nonzero hyperfine fields in their Mössbauer spectra at almost the same temperature that the irreversibility in thermomagnetic measurements appeared, suggesting a single sharp transition to an asperomagnetic state.

In spite of the evidence for homogeneous transverse spin freezing in a-Fe-T alloys, two inhomogeneous models have been proposed.[24,25] Both assume a FM matrix phase, with either AF (Ref. 24) or FM (Ref. 25) clusters embedded in it. In both cases T_c marks the ordering of the matrix phase, while the second transition corresponds to the ordering of the clusters. Frustration at the cluster surfaces destroys the long-range FM order established at T_c and leads to spin-glass behavior.

We present here Mössbauer and magnetization data on iron-rich glasses containing Sc, Zr, and Hf. The emphasis is on the consistent evolution of the complete a-Fe-T system as a function of composition. We can adjust the degree of frustration present by changing the composition and thus study how a group of systems evolves from ferromagnet to spin glass as we increase frustration. Three models for the behavior are examined in detail, and two invoking magnetic clusters are found to be inconsistent with the data. Finally, a quantitative comparison is made with numerical simulations.

II. EXPERIMENTAL METHODS

Ribbons of a-Fe-Zr, a-Fe-Hf, and a-Fe-Sc alloys were melt spun under helium from ingots prepared from the pure metals (99.95%, or better) by arc melting under Ti-gettered argon. The absence of crystallinity was confirmed by x-ray diffraction and room-temperature Mössbauer spectroscopy. Compositions were checked by electron microprobe analysis, and were found to be within 0.3% of nominal in all cases.

Mössbauer spectra were obtained over a temperature range from 5 K to room temperature on a conventional constant acceleration spectrometer with a 1 GBq ^{57}CoRh source normally at room temperature. High-field spectra were recorded with an external field applied parallel to the γ beam using a superconducting solenoid. For these measurements, the source was located inside the cryostat at the null point of the megnet and the spectrometer was operated in sinusoidal mode. The field was applied above T_c and the spectra were obtained following field cooling.

Most spectra were fitted using Window's method, where no assumptions about the shape of hyperfine field distribution, $P(B_{hf})$, are made.[26] We also used a simple fixed-shape distribution constructed from two half-Gaussians with a common peak, and different widths to high and low fields. This form cannot oscillate, requires only three parameters to describe $P(B_{hf})$, and yields average parameters that are indistinguishable from those derived from Window's method. The spectra of a-$Fe_{89}Zr_{11}$ and a-$Fe_{90}Zr_{10}$, measured in a large applied field, were fitted using the $P(B_{hf})$ obtained by a subtraction procedure.[27] Polarizing the sample with a 100 mT field applied perpendicular to the direction of the γ beam leads to an increase in the intensity ratio (R) of lines 2 and 5 relative to lines 3 and 4, often to as much as 3.7 (compared with the powder average value of 2, and the maximum possible of 4). Subtracting the zero-field spectrum from the one obtained in 100 mT yields a two-line spectrum with essentially no line overlap that can be fitted easily. $P(B_{hf})$ derived from the difference spectrum at a given temperature was checked by using it to fit the original polarized and unpolarized spectra. This procedure is described in more detail elsewhere.[20]

The total iron moment and hyperfine field are assumed to be directly proportional to each other. The conventional conversion factor of $15T/\mu_B$, found in α-Fe and many intermetallic compounds, has been used here. The agreement obtained for the collinear a-$Fe_{89}Zr_{11}$ alloy and above T_{xy} for the other alloys studied here supports this choice of conversion factor. For Mössbauer spectra measured in an external field, the additional contribution, corrected for the demagnetizing field, was included when calculating $\langle B_{hf} \rangle$.

Mössbauer ordering temperatures were determined both from the point at which the average hyperfine field first became nonzero, and from the change in absorption at zero velocity as a function of temperature (the thermal scan technique). T_{xy}, which marks the onset of noncollinearity, was identified as the temperature at which the intensity of lines 2 and 5 (R) first becomes nonzero in the applied field Mössbauer spectra. In the absence of a better model, the intercept of a linear fit to R vs T was used. We note that our values for T_{xy} are obtained in an internal field of ~ 2 T; however, the field dependence of this transition is either zero[3,28] or at worst <0.8 K/T,[29] and thus any possible field induced shift in T_{xy} is negligible in comparison with the measurement uncertainties.

Magnetization measurements were made between 5 and 300 K on a Quantum Design superconducting quantum interference device (SQUID) magnetometer in fields of up to 5.5 T, and calibrated using a Pd standard. Magnetization ordering temperatures were determined from modified Arrott plots: $M^{1/\beta}$ vs $(B/M)^{1/\gamma}$, by identifying the isotherm that passed through the origin. Values for the critical exponents β and γ obtained from magnetiza-

tion measurements on a-Fe-Zr (Refs. 30 and 31) have been shown to agree well with theoretical predictions for the homogeneous three-dimensional Heisenberg model[32] where $\beta=0.365$ and $\gamma=1.387$. We have therefore used these values here, and found them to yield reasonable isotherms.

III. RESULTS

We present here the results of Mössbauer and magnetization measurements used to probe local and large-scale magnetic ordering, respectively. Each sample has been studied from above its ordering temperature down to 5 K. The agreement between ordering temperatures derived from modified Arrott plots and Mössbauer data shows that magnetic order develops simultaneously on long and short length and time scales. Comparison of Mössbauer and magnetization derived moments along with applied field Mössbauer data allows us to determine T_{xy}, the temperature below T_c at which noncollinearity develops, and to show that long-range ferromagnetic order is not lost at any lower temperature. The a-Fe-Zr samples studied here span the full range of behavior accessible to melt-spinning in this system. One a-Fe-Hf sample is included for comparison with the zirconium alloy series, while the a-Fe-Sc sample serves as an example of complete exchange frustration, and provides a severe test of the various ordering models proposed for these alloys.

a-Fe_xZr_{100-x}

a-$Fe_{89}Zr_{11}$ shows magnetization behavior typical of conventional ferromagnets (top of Fig. 1), reaching 92% of saturation (extrapolation of M vs $1/B$ plot to $1/B=0$) in a field of 0.1 T. Modified Arrott plots (bottom of Fig. 1) yield straight isotherms, and indicate an ordering temperature of 255±5 K, in good agreement with the onset of magnetic splitting in the Mössbauer spectra at 252±5 K. M_z, a measure of the component of the iron moment parallel to the field direction, is obtained by extrapolating the high-field part (2 T$\leq B \leq$5.5 T) of the magnetization curves to $B=0$ T. The average total iron moment (μ_{av}) can be obtained from the average hyperfine field, $\langle B_{hf}\rangle$, derived from Mössbauer spectra, using the conversion factor of $15T/\mu_B$. A comparison of these two parameters in Fig. 2 shows that μ_{av} and M_z are indistinguishable at all temperatures, indicating collinear ordering down to 5 K, and confirming the choice of conversion factor. Mössbauer spectra measured in a 3.5 T field parallel to the γ beam are shown in Fig. 2. The six lines observed in a magnetically split spectrum have intensities 3:R:1:1:R:3, where $R=4\sin^2\theta/(1+\cos^2\theta)$, and θ is the angle between the magnetic moment and the direction of γ beam. There is no evidence of the presence of lines 2 and 5 at any temperature, indicating that the magnetic order remains collinear down to 5 K. Since a-$Fe_{89}Zr_{11}$ is the least frustrated sample among the a-Fe-Zr group studied here, it is possible that it does not have two magnetic transitions. In order to check this, we need to obtain accurate values for R at different temperatures using the subtraction procedure described earlier. $P(B_{hf})$ obtained by this method at 5 K has been used to fit the spectrum recorded in 3.5 T at the same temperature. Since the shape of $P(B_{hf})$ is fixed, only R and a field shift remain as adjustable parameters. The latter takes account of the applied field, which reduces the hyperfine field at the iron nucleus. $R=0.04\pm0.01$ was obtained from this procedure at 5 K. However, there was no statistically significant difference in the fit quality with $R=0.04$ compared to that with R constrained to be zero (both lines are shown in Fig. 2).

Mössbauer and magnetization measurements indicate that a-$Fe_{89}Zr_{11}$ exhibits conventional ferromagnetic behavior down to 5 K. The evidence includes the agreement between the magnetization and the average hyperfine field (which indirectly confirms the choice of conversion factor), and absence of intensity in lines 2 and 5 at any temperature. The ordering is indistinguishable from collinear down to 5 K in this alloy, and no evidence of a second transition is observed.

As the Zr content of the alloys is reduced, this simple behavior changes. First, while modified Arrott plots and Mössbauer thermal scans continue to yield T_c values in agreement with each other, the actual values obtained

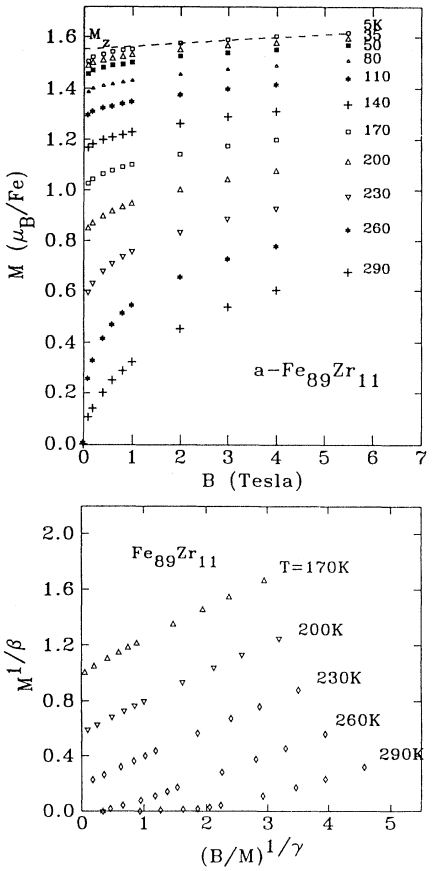

FIG. 1. Top: magnetization curves for a-$Fe_{89}Zr_{11}$ at various temperatures. Dotted line shows definition of M_z at 5 K. Bottom: modified Arrott plots from which a T_c of 255±5 K is deduced.

TABLE I. Basic magnetic parameters for the a-Fe-T alloys studied here. Average hyperfine field $\langle B_{hf} \rangle$ at 5 K, ferromagnetic ordering temperatures (T_c) determined from Mössbauer spectroscopy and modified Arrott plots, and onset of noncollinearity T_{xy}.

Sample	$\langle B_{hf} \rangle$ at 5 K (T)	T_c Mössb. (K)	T_c Arrott (K)	T_{xy} (K)
$Fe_{89}Zr_{11}$	23.4±0.2	252±5	255±5	< 5
$Fe_{90}Zr_{10}$	23.0	230	230	28±3
$Fe_{92}Zr_7Sn$	23.7	180	190	46±8
$Fe_{93}Zr_7$	23.3	140	150	78±8
$Fe_{92.5}Hf_{7.5}$	22.7	175	186	47±8
$Fe_{91}Sc_9$	22.1	105	< 5	97±10

(summarized in Table I) fall rapidly, reflecting increasing exchange frustration. Second Mössbauer spectra recorded in a field applied parallel to the γ direction show signs of intensity in lines 2 and 5 at 5 K [see, for example, the spectra in Fig. 3 (Ref. 33)] reflecting the development of a noncollinear spin structure. The intensity and hence the degree of noncollinearity (summarized in Table II) increases as the Zr content is reduced. Third, the average

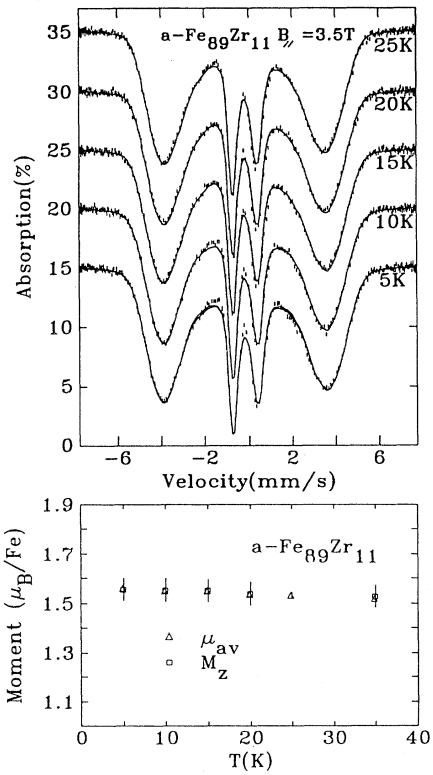

FIG. 2. Top: Mössbauer spectra for a-$Fe_{89}Zr_{11}$ at various temperatures measured in an applied field of 3.5 T. The absence of lines 2 and 5 at all temperatures confirms the collinear ordering. Bottom: comparison of μ_{av}, derived from Mössbauer spectra, with M_z, derived from magnetization measurements at various temperatures. Close agreement supports choice of 15 T/μ_B conversion factor, and shows that the order is collinear.

TABLE II. Characteristics of transverse spin freezing behavior in the a-Fe-T alloys studied here. Onset of noncollinearity, intensity of Δm_I transitions in applied field spectra (R), ratio of magnetization to average moment (M_z/μ_{av}), cone half-angle derived from Mössbauer data in an applied field (ψ_R) and from comparison between Mössbauer and magnetization data (ψ_M).

Sample	T_{xy} (K)	R	M_z/μ_{av}	ψ_R (deg)	ψ_M (deg)
$Fe_{89}Zr_{11}$	< 5	< 0.04	1.00	0	0
$Fe_{90}Zr_{10}$	28±3	0.14±0.01	0.98	22±1	17±4
$Fe_{92}Zr_7Sn$	46±8	0.35±0.04	0.85	34±3	38±4
$Fe_{93}Zr_7$	78±8	0.53±0.04	0.72	42±3	55±4
$Fe_{92.5}Hf_{7.5}$	47±8	0.25±0.04	0.88	29±3	30±4
$Fe_{91}Sc_9$	97±10	0.73±0.05	0.55	50±3	69±4

moment μ_{av} and the magnetization M_z no longer agree at 5 K (Fig. 3) and this difference increases as the Zr content is reduced, as does the intensity observed in lines 2 and 5 (compare Figs. 3 and 4). If we consider a highly idealized asperomagnetic model, where the iron moments are distributed randomly within a cone of half-angle ψ,[34] then we can obtain two different estimates for the degree of noncollinearity present at 5 K by combining the Mössbauer and magnetization data. ψ_R is derived directly from the fitted intensity of lines 2 and 5, while ψ_M is obtained from the ratio of M_z and μ_{av}. The results of this analysis (Table II) show that while ψ_M is always larger than ψ_R, the values agree within error. It is unlikely that the small systematic differences are significant, in part because of the highly idealized nature of the model, but also because of the way in which the two methods sample noncollinear spin structures. A small number of spins rotated by more than 90° from the z axis will greatly reduce the magnetization, but the $\cos^2\theta$ dependence of R on θ means that spins making an angle $90°+\theta$ with the z axis are equivalent to those at $90°-\theta$, so that reversed spins contribute little to R. Small numbers of antiparallel spins have been observed in Monte Carlo simulations of frustrated Heisenberg systems,[35] and the presence of almost inverted spins could easily account for the greater apparent noncollinearity derived form M_z/μ_{av} in the more frustrated alloys.

Examination of Figs. 3 and 4 shows that the noncollinearity described above is not present at all temperatures. It is absent at higher temperatures, immediately below T_c (R is zero, and $M_z=\mu_{av}$), and develops at a well-defined temperature, T_{xy}, significantly below T_c. At T_{xy}, the transverse spin components, while precess rapidly and time average to zero between T_c and T_{xy}, freeze in random orientations perpendicular to the bulk magnetization. They contribute both to R, as they are perpendicular to the γ beam, and to μ_{av}, because the total ordered moment increases, but not to M_z, as the increase occurs perpendicular to the z axis and its direction changes randomly from site to site. T_{xy} can be obtained from either the point at which μ_{av} first exceeds M_z, or more accurately, from the temperature at which $R \neq 0$. The two values

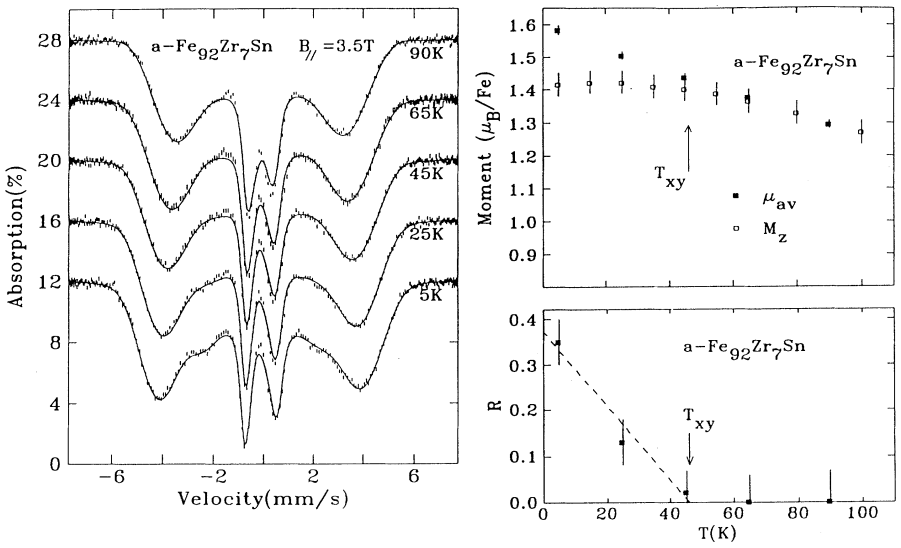

FIG. 3. Left: Mössbauer spectra for a-$Fe_{92}Zr_7Sn$ at various temperatures measured in an applied field of 3.5 T. The development of intensity in lines 2 and 5 by 5 K is clearly visible. Top right: Comparison of μ_{av} with M_z. Separation at $T_{xy}=46$ K marks the ordering of transverse spin components. Bottom right: Temperature dependence of intensity in lines 2 and 5 showing development of noncollinearity at T_{xy}.

agree, and only those derived from $R(T)$ are given in Table II. T_{xy} rises rapidly with Fe content as T_c falls.

$Fe_{92.5}Hf_{7.5}$

The iron-rich a-Fe-Hf alloy system has been shown to be magnetically similar to a-Fe-Zr.[11,23] The sample presented here serves as an example of a significantly frustrated alloy that does not contain Zr, in order to demonstrate that the results are not dependent on a particular alloying element. The composition chosen represents the maximum iron content that we were able to obtain in a fully amorphous state by melt spinning.

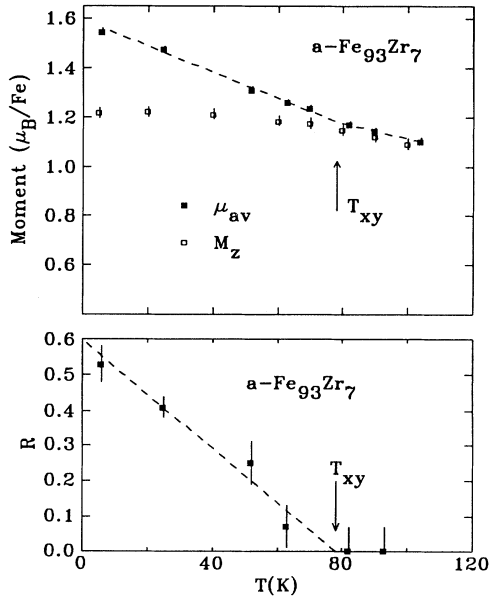

FIG. 4. Top: Comparison of μ_{av} with M_z for a-$Fe_{93}Zr_7$ at various temperatures. Separation at $T_{xy}=78$ K marks the ordering of transverse spin components. Bottom: Temperature dependence of intensity in lines 2 and 5 showing development of noncollinearity at T_{xy}.

Modified Arrott plots give an ordering temperature of 186±7 K in agreement with the onset of magnetic splitting at 175±5 K. The difference between μ_{av} and M_z begins to increase around T_{xy}, showing behavior typical of transverse spin freezing. Mössbauer spectra measured in a 3.5 T field applied parallel to the γ beam show the presence of lines 2 and 5 at low temperatures. T_{xy} is determined to be 47±8 K. Since T_c and T_{xy} of a-$Fe_{92.5}Hf_{7.5}$ are both close to those for a-$Fe_{92}Zr_7Sn$ (Table I), we expect the frustration level and therefore the spin structures below T_{xy} to be quite similar for the two samples. R is 0.25±0.04 at 5 K, corresponding to a cone half-angle, ψ_R, of 29±3° while ψ_M is 30±4°. As expected, these values are similar to those obtained for a-$Fe_{92}Zr_7Sn$ (Table II).

$Fe_{91}Sc_9$

Iron-rich a-Fe-Sc exhibits significantly lower ordering temperatures than any of the other alloy systems studied here.[6,7] Furthermore, analysis of χ_{ac} data has suggested that the system is almost completely frustrated[15] and therefore almost a spin glass. The sample serves here as an example of extreme frustration leading to a complete loss of collinear order.

Magnetization curves for a-$Fe_{91}Sc_9$ (top of Fig. 5) show the largest high-field slopes of all of the materials studied here, consistent with it being the most frustrated system. M_z is compared with μ_{av} in Fig. 6. Even above the ordering temperature (105±3 K), both μ_{av} and M_z are nonzero due to the slowing down of cluster relaxation by external fields.[36] μ_{av} is consistently larger than M_z as the Mössbauer measurements include contributions from clusters relaxing too rapidly to be seen by magnetization. Furthermore, the applied field Mössbauer spectra (see below) show that the magnetic order in this alloy is noncollinear at all temperatures. M_z appears to be only weakly temperature dependent, increasing by only about 10% from the χ_{ac} ordering temperature of 105 K down to

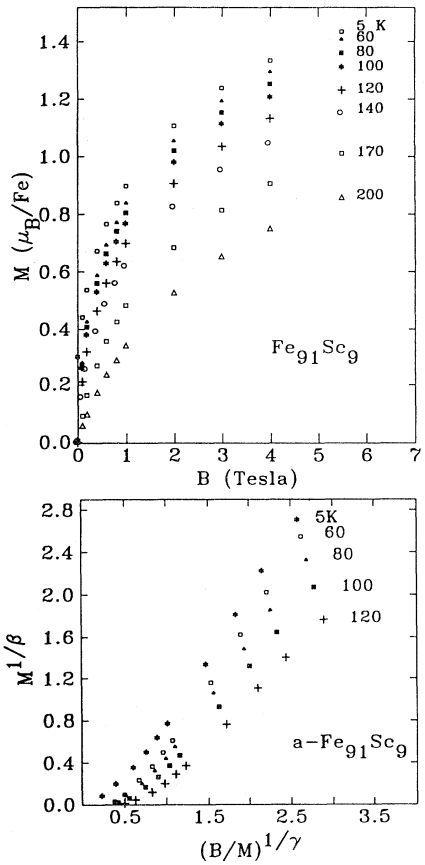

FIG. 5. Top: magnetization curves for a-$Fe_{91}Sc_9$ at various temperatures. Note the severe high-field slopes and curvature. Bottom: modified Arrott plots. No spontaneous magnetization is observed at any temperature and therefore no ordering temperature can be deduced for this severely frustrated material using this method.

5 K. The ratio of M_z to μ_{av} at 5 K is 0.55, suggesting a higher degree of noncollinearity than in any of the other materials studied here (Table II). Since nonzero values for M_z were obtained at all temperatures from 5 to 200 K, it might seem that the ground state is asperomagnetic, characterized by severe noncollinearity but a finite magnetization. However, M_z was obtained by extrapolation of the high-field part (2 T $\leq B \leq$ 5.5 T) of the magnetization curves, and such fields could cause significant changes in magnetic structure. This is most clearly seen in Fig. 6 where M_z is nonzero even well above the ordering temperature determined from Mössbauer spectroscopy and χ_{ac}. Although M_z is an extrapolation to $B=0$ T, it includes contributions induced by the large magnetic fields. We therefore turn to the low-field part of the magnetization curves. The modified Arrott plots shown in Fig. 5 are quite unlike any of those obtained for the other alloys in this study. Although there is some residual curvature, suggesting that the scaling is not quite correct, their form is reasonable. However, they yield no ordering temperature, a result that stands in stark contrast to those obtained on the other alloys in this study (Table I), where good agreement between magnetization and Mössbauer derived ordering temperatures was obtained. More significantly, it is clear that there is no spontaneous magnetization apparent at any temperature. The values of M_z in Fig. 6 are therefore artifacts of the large fields used to obtain them.

The temperature dependence of the average hyperfine field obtained from Mössbauer spectra measured in zero field for a-$Fe_{91}Sc_9$ yields an ordering temperature of 105±3 K. Mössbauer spectra in a 6 T field applied parallel to the γ beam are shown in Fig. 6. The external field has strong effects on the magnetic structure of the sample. Above the ordering temperature, the spectra measured in an applied field clearly exhibit a substantial mag-

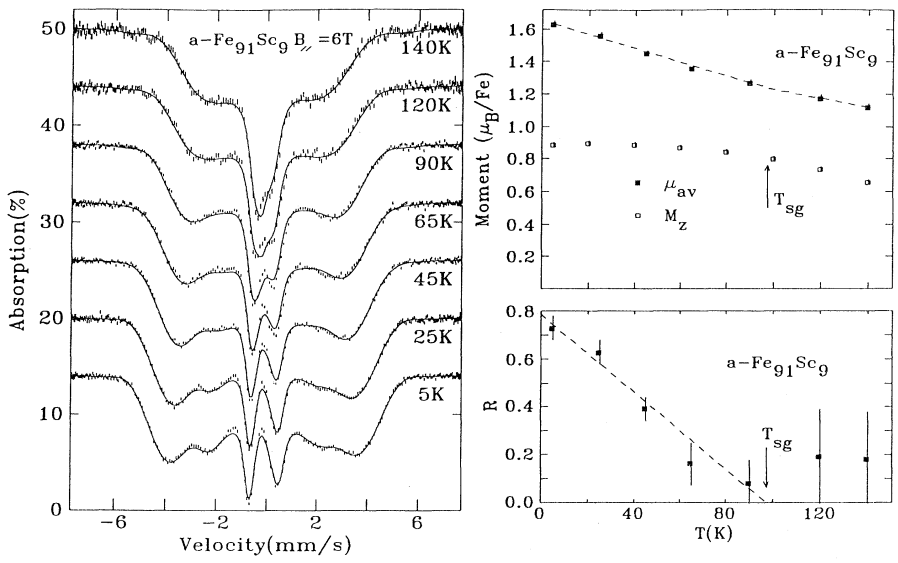

FIG. 6. Left: Mössbauer spectra for a-$Fe_{91}Sc_9$ at various temperatures measured in an applied field of 6 T. Note the persistence of magnetic splitting above $T_{sg}=105$ K, and the presence of intensity in lines 2 and 5 at all temperatures below T_{sg}. Top right: comparison of μ_{av} with M_z. Both parameters are large, even above the ordering temperature of 105 K, and there is substantial disagreement between the Mössbauer and magnetization results reflecting severely noncollinear order. Bottom right: temperature dependence of intensity in lines 2 and 5 showing that onset of noncollinearity at 97 K coincides with development of order at 105 K.

netic splitting, and average hyperfine fields of more than 10 T are obtained, providing evidence of significant magnetic cluster relaxation. From Fig. 6, it can also be seen that the intensities of lines 2 and 5 increase at low temperatures. The applied field spectra were fitted using Window's model since the subtraction procedure does not work for this system. The fitted values of R are plotted against temperature in Fig. 6. The temperature at which R begins to increase from zero has been estimated by fitting the temperature dependence of R with a linear function to yield 97 ± 10 K, implying that the noncollinearity starts to develop as soon as magnetic order appears. Therefore, unlike the a-Fe-Zr and a-Fe-Hf alloys, which first enter a collinear state at T_c and develop noncollinearity only below the second transition at T_{xy}, a-$Fe_{91}Sc_9$ undergoes a single magnetic transition and enters a noncollinear state directly. Despite the fact that Mössbauer[7] and susceptibility[6] measurements clearly show that magnetic order appears at around 105 K, the modified Arrott plots shown in Fig. 5 show no evidence of a spontaneous magnetization at any temperature above 5 K. We therefore conclude that a-$Fe_{91}Sc_9$ undergoes a transition to a spin glass rather than to an asperomagnetic state at 105 K, and label the transition temperature T_{sg} rather than T_c in Fig. 6.

IV. DISCUSSION

We gather our major results on the a-Fe-Zr system together in Fig. 7. There are three specific effects clearly visible. (i) With increasing iron concentration T_c falls by a factor of 2. Since there is no reduction in the average iron moment, the exchange distribution in the system must be changing substantially. (ii) A second magnetic transition appears, and rises to meet the descending T_c line. In the same composition range that T_c falls by 130 K, T_{xy} rises by 80 K. (iii) The materials become increasingly noncollinear, with ψ rising from 0° to nearly 60°. Our evidence of noncollinearity comes primarily from the direct observation of intensity in lines 2 and 5 of Mössbauer spectra recorded in magnetic fields applied parallel to the γ beam. It is backed up by a less direct measure of the spin structure, namely a comparison of the longitudinal component of the magnetization M_z with the average iron moment derived from $\langle B_{hf}\rangle$. Not only does M_z separate from μ_{av} at the same temperature (T_{xy}) at which R ceases to be zero, but the degree of noncollinearity derived from M_z/μ_{av} agrees with the direct observation using R.

Ruling out of cluster models

There are two competing inhomogeneous models which invoke magnetically distinct clusters to explain the magnetic ordering in iron-rich amorphous Fe_xT_{100-x} alloys. Both assume the presence of a ferromagnetically coupled matrix phase which orders at T_c, and forms the bulk of the material. The large, possibly divergent, susceptibility at T_c and the substantial magnetization below T_c make any other matrix phase unlikely. The models differ, however, in the nature of the cluster phase proposed.

One model, due to Read *et al.*[24,37] assumes that antiferromagnetic γ-iron–like precipitates are dispersed throughout the sample, these order at a lower temperature, and random-field effects at their surfaces destroy the previously established FM order. Proponents of this FM-AF model point to the fact that the probability that an iron atom, in a close-packed alloy that is 90% iron, will have only iron neighbors is of order 30%, implying that a large fraction of the iron could be in γ-Fe–like environments. The fortuitous agreement between the Néel temperature of γ-Fe precipitates in Cu [$\sim$70 K (Ref. 14,38,39)] and T_{xy} in a-$Fe_{93}Zr_7$ (78 K, this work and Ref. 18) is seen as supporting the FM-AF model; however, as is clear from Fig. 7, this agreement occurs only for a single composition.

Another model (FM-FM), due to Kaul *et al.*,[25,40] identifies the clusters with density fluctuations. Lower density regions are more strongly FM coupled than the matrix, but isolated from the matrix by a boundary layer of frustrated spins. The boundary frustration arises both from magnetostrictive effects due to lattice mismatch between the cluster and matrix phases, and also from shorter Fe-Fe contacts, i.e., the boundary layer is assumed to be denser than either the matrix or the cluster phases. The FM clusters account for both the relaxation behavior seen at T_c, and the short correlation lengths seen in small-angle neutron-diffraction measurements.[41] The matrix orders ferromagnetically at T_c, but thermal fluctuations overcome the weak cluster-matrix coupling and prevent the clusters from affecting the matrix order. At T_{xy}, the clusters finally couple to the matrix, and the random influences of the frustrated surface bonds destroy the FM order in the matrix.

There are two key features common to both models. (i) two distinct spin populations with different ordering behaviors, and (ii) the destruction of the FM order at the second transition (T_{xy}). As we will now show, cluster-

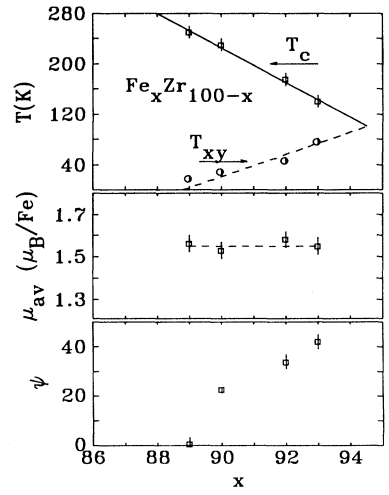

FIG. 7. Summary of the magnetic behavior of a-Fe_xZr_{100-x} as a function of composition. Top: magnetic transition temperatures T_c and T_{xy}. Center: average magnetic moment. Bottom: the cone half-angle ψ showing the increasing noncollinearity of the order.

based explanations suffer from several basic problems. First, and perhaps most serious, there is no direct observational evidence for the existence of isolated, or distinguishable, magnetic clusters. Second, neither model is consistent with the composition dependence visible in the phase diagram shown in Fig. 7. Third, they cannot explain the extreme behavior of *a*-Fe-Sc. Finally, it is difficult to reconcile the effects of hydrogen with either model.

Direct searches by small-angle scattering of neutrons (SANS) or x-rays (SAXS) do not yield support for the cluster models. In general, SAXS has shown metallic glasses to be extremely uniform,[42] and in particular, SANS measurements on *a*-Fe-Zr alloys found no evidence of inhomogeneities.[43] Indeed, the only parameter consistently cited as showing evidence for clusters in these materials is the distribution of hyperfine fields, $P(B_{\rm hf})$, obtained by deconvoluting Mössbauer spectra, a process that frequently yields bimodal forms—the main peak is then attributed to the matrix, while the smaller, lower-field feature is due to the clusters. However, both we[20] and others[44] have noted that the form of the hyperfine field distribution is essentially temperature independent, if sufficient care is taken in the analysis, an observation that is totally inconsistent with the separate ordering of two distinct magnetic components. Furthermore, a direct test for the presence of magnetically isolated clusters is possible. The subtraction method used to fit some of the spectra presented here, relies on being able to polarize the whole sample. The difference spectrum obtained by subtracting an unpolarized spectrum from one obtained in $\sim$100 mT only contains contributions from moments that changed direction when the field was applied, and thus changed their contribution to lines 2 and 5. If some of the spins are not affected by the applied field, because they are part of either AF clusters, or decoupled FM clusters, they will not be represented in the two-line difference spectrum. A fit to the two-line spectrum should then lack the low-field feature in $P(B_{\rm hf})$, if it were genuinely associated with cluster moments, and the hyperfine field distribution obtained in this manner should not fit one or both of the original spectra. The cluster component is predicted to be substantial, ranging from $\sim$20% (Ref. 24) to $\sim$30% (Ref. 25) in *a*-$Fe_{90}Zr_{10}$ for example, and therefore the misfit due to omitting so large a cluster contribution should be severe. However, unpolarized spectra obtained above and below T_{xy} for this composition are shown in Fig. 8 with subtraction-derived fits and residuals. It is apparent first that there is no change in the misfit observed above and below T_{xy}, and second, that any misfit is small, and certainly represents far less than 20% of the total area. Therefore, the magnetic system responds homogeneously to small applied fields both above and below T_{xy} and no evidence for clusters is found.

Since $P(B_{\rm hf})$ is so widely quoted in support of clusters, it is essential that the limitations of the deconvolution procedures used be emphasized. The most obvious problem is line overlap.[45] It is readily apparent from an examination of any of the spectra shown in this work that lines 2 and 5 overlap significantly with lines 1 and 6

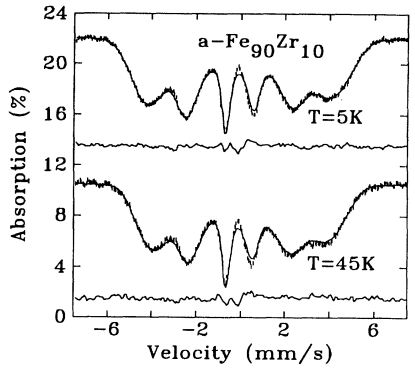

FIG. 8. Zero-field Mössbauer spectra for *a*-$Fe_{90}ZR_{10}$ measured above and below T_{xy}. The solid lines through the data are fits derived from the subtraction technique described in the text. The residuals from these fits are shown below each spectrum. Note the absence of any misfit that could be associated with isolated magnetic clusters.

which lie outside them. Since all of the distributions of $B_{\rm hf}$ for the magnetically ordered alloys considered here exhibit some form of tail to low fields, all of the lines exhibit some asymmetric broadening to low velocities (i.e., towards the center of the spectrum). Thus some of the area in the region of line 2 (for example) is due to the low velocity tail of line 1 and the rest is due to line 2. In order to determine the actual form of the low-field part of $P(B_{\rm hf})$ it is necessary to know the correct intensity of lines 2 and 5. The $\Delta m_I=0$ transitions that yield lines 2 and 5 have intensities (R) which depend on the orientation of the moments with respect to the γ beam (a feature used here to show that the order is noncollinear). The moment directions are rarely known with any certainty as they are affected by stray fields and stresses introduced during preparation, they can also change with temperature as differential contractions of the sample and mount cause further stresses. For simplicity, a random distribution of moment directions is often assumed, with R being taken as 2. However, the subtraction method described above has been used to show that such assumptions can be seriously wrong: analysis of the difference spectra for *a*-$Fe_{90}Zr_{10}$ showed that R was close to 1 in unpolarized spectra.[20] It is not possible to determine the shape of the low-field part of the hyperfine field distribution without knowing the exact intensities of the $\Delta m_I=0$ transitions (or vice versa). This consideration alone makes the detailed form of the low-field tail in $P(B_{\rm hf})$ essentially impossible to determine from a single spectrum at a given temperature.

Even without the ambiguity due to line intensity problems, the deconvolution procedures commonly used are unstable, and will naturally tend to oscillate. This problem is certainly exacerbated by poor counting statistics (i.e., noise on the data); however, the extent of the tendency to oscillate is not fully appreciated. In order to demonstrate, we show some synthetic spectra in Fig. 9. The spectra were generated using the distributions at the left, which are asymmetric Gaussians as discussed earlier. The degree of asymmetry increases from top to bottom,

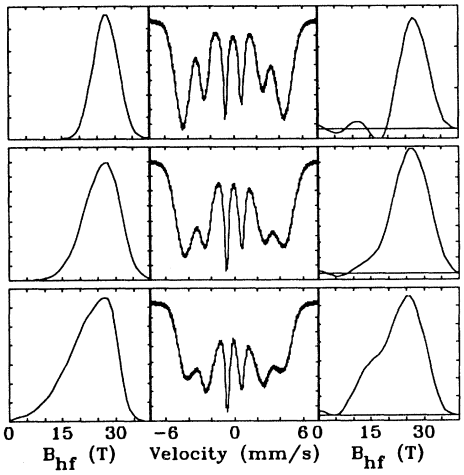

FIG. 9. Synthetic Mössbauer spectra showing the instability of deconvolution procedures. In each case, the hyperfine field distribution at the left gives the spectrum in the center, which when fitted with a six-term Window expansion yields the distribution at the right. Note how as the low-field tail of the original distribution becomes more pronounced, an artificial bimodal structure develops in the fitted distribution.

and spans typical values encountered in a-Fe-Zr. At the right are the distributions obtained by fitting six-term Window expansion[26] to the spectra. The "bimodal" structure is clearly visible, despite its absence from the original data. The bimodality could not have been caused by noise, as none was added to the synthetic spectra. It is entirely mathematical in origin.

The fitting procedures are fundamentally unstable, even when used on perfect, noise-free data, and yield bimodal distributions that are absent from the original data. Thus any discussion of such features extracted from real spectra with noise present is invalid. Direct searches for chemical or magnetic inhomogeneities yield negative results. There is therefore no experimental evidence for the existence of magnetically distinct clusters in any of the alloys considered here.

The second problem with cluster models is the observed phase diagram. Both the composition dependence of the transition temperatures and the magnetic structure below T_{xy} are inconsistent with cluster-based models. The FM-matrix–AF-cluster model works only for a-$Fe_{93}Zr_7$, in that it predicts the correct value for T_{xy}. However, as the second transition is assumed to be due to γ-Fe–like regions, the model can only yield a single value for T_{xy}, namely T_N of γ-Fe: $\sim$70 K. There is no obvious reason for T_N to vary with the composition of the matrix, and certainly none that would cause the transition to move from 0 K to nearly 80 K as the Zr content changes by 4 at. %. Furthermore, the model provides no mechanism by which T_c of the matrix phase may be changed.

Similar problems exist with the FM-FM model. If the density fluctuations were significant, they would presumably exist on all length scales and with varying amplitudes, making the distinction between "cluster" and "matrix" problematic. There is no direct structural evidence for either density or compositional fluctuations in these glasses; indeed careful x-ray-diffraction measurements of a-Ni-Zr show no difference between the structure factors of melt-spun and sputtered alloys, despite extreme differences in preparation conditions.[46] While it is known that as-cast glasses contain quenched-in stresses and free volume that can be released on annealing,[47] the slight densification on thermal relaxation has been shown to result from highly dispersed motions, rather than local elimination of poor packing, an observation that does not support the existence of well-defined low-density regions. Furthermore, the degree of densification observed on annealing is critically dependent on the preparation conditions,[48] which would mean that the density fluctuations present in a sample would depend on its detailed thermal history or preparation conditions. However, the magnetic phase diagram of a-Fe-Zr is remarkably consistent. T_{xy}, which would be extremely sensitive to variations in the cluster density and/or amplitude if they caused the second magnetic transition, shows little variation from group to group, even when radically different methods are used to determine it. Figure 10 shows a comparison of T_{xy} values from different sources, showing that despite varying sample preparation conditions, differing measuring techniques and views on the origin of the feature, its location is remarkably stable; indeed, most of the scatter visible in Fig. 10 could be accounted for by $\sim$0.3 at. % variations in sample composition. As with the FM-AF model, there is no mechanism for changing either T_c or T_{xy} in the FM-FM model. It is not clear why density fluctuations should become so much more significant over a narrow composition range, why the ordering temperature of the matrix phase should drop with increasing iron content, or why the clusters should order at progressively higher temperatures as the ordering temperature of the matrix falls.

Both the FM-AF and FM-FM cluster models predict that, as a result of frustrated interactions on the cluster

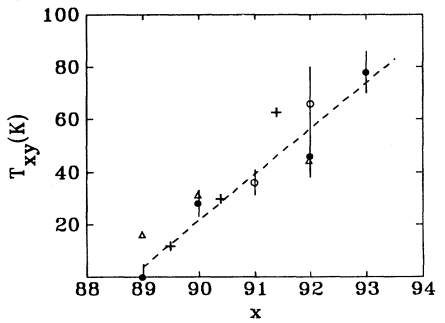

FIG. 10. Comparison of T_{xy} values derived from various sources. ●, this work; △, χ_{ac} data (Ref. 67); +, χ_{ac} measured with superposed dc field (Ref. 17); ○, χ_{ac} data (Ref. 68). The dotted line is a linear fit to our data. Note that although our values were obtained in fields of order 2 T, they are not systematically shifted from the zero-field results also shown here. Any field-induced shift in T_{xy} is therefore small.

surfaces, the ferromagnetic order established at T_c is lost when the clusters freeze. This prediction is inconsistent with the experimental observation that domains persist down to 14 K (well below T_{xy}) in a-Fe_xZr_{100-x} ($89 \leq x \leq 92$),[49,50] and that the only effect of the transverse spin freezing at T_{xy} on the domain structure is to reduce domain-wall mobility. Furthermore, neutron depolarization measurements confirm that ferromagnetic order is not lost at, or below T_{xy}.[51] Not only do the cluster models lack a mechanism to account for the observed composition dependence of the transition temperatures, but they also predict a loss of ferromagnetic order at T_{xy}, contrary to direct experimental observations.

a-Fe-Sc provides a third problem for the cluster models. The magnetic ordering behavior of a-$Fe_{91}Sc_9$ appears quite different from that of the a-FeZr and a-Fe-Hf alloys also studied here. Our results indicate that it exhibits a single transition to a noncollinear ordered state with no spontaneous magnetization. Within cluster models of the ordering, $M_z = 0$ implies that the ferromagnetic matrix is essentially absent. Leaving aside the fact that both models require a matrix phase to define the clusters, and that there is no obvious reason for the arguments leading to a cluster-matrix separation to change when Sc is substituted for Zr, we will examine the model predictions for this situation.

In the FM-AF model, the system would have to consist entirely of γ-Fe, unlikely in view of the 9 at. % Sc present in the alloy. A T_N of $\sim$70 K might be expected, and as the matrix phase is absent, $P(B_{hf})$ should only show the low-field γ-Fe component at 10 T,[24] rather than the much larger value of 22.1 T actually observed.[6,7] Indeed, Table I shows that the average hyperfine field in a-Fe-Sc is only slightly smaller than that in the corresponding a-Fe-Zr alloy. If we try to include a FM matrix phase, then the ordering temperatures of the matrix phase and the γ-Fe clusters are required to match within a few degrees, so that the clusters can destroy the order in the FM matrix as soon as it develops. There is no natural way for this remarkable coincidence to arise.

Eliminating the matrix phase from the FM-FM model leads to two possible results: (i) the cluster component accounts for all of the sample volume, in which case the system is entirely ferromagnetic with a T_c given by the (assumed stronger) coupling within the now infinite cluster phase; (ii) the boundary frustration remains and the system consists almost entirely of clusters, isolated from each other by thin layers of frustrated spins. In either case, $P(B_{hf})$ must be dominated by the low-field component at 15 T,[25] a prediction that is again inconsistent with observations.[6,7] Possibility (i) can be discounted immediately as it predicts an enhanced T_c and FM ordering. The isolated cluster case (ii) could, in principle, account for the noncollinear ordering if the behavior at T_{sg} is identified with the blocking of isolated superparamagnetic clusters; however, this does not stand up to closer examination, with measurements on very different time scales giving almost identical values for the transition temperature. ^{57}Fe Mössbauer spectroscopy, which is sensitive on a time scale of $\sim 10^{-7}$ s, gives $T_{sg} = 105 \pm 3$ K compared with 99 K (Ref. 6) and 95 K (Ref. 15) derived from χ_{ac} measurements, where a driving field of several kHz was used, while we have obtained a value of 102 ± 3 K at 137 Hz. If the ordering were due to blocking of isolated clusters, measurements over such a frequency range should yield transition temperatures that change by a factor of 2.[52]

While a-Fe-Sc exhibits quite strong superparamagnet-like effects, and might be expected to represent the limiting case for the cluster models, neither model is consistent with the observed magnetic ordering behavior. In particular, $P(B_{hf})$, which is often cited as showing the existence of clusters in a-Fe-Zr, does not indicate that the supposed cluster component of the distribution dominates in a-Fe-Sc.

The effect of hydrogen provides a final problem for the cluster models. It is well known that adding hydrogen to a-Fe-T alloys raises T_c and converts them into collinear ferromagnets,[7,10,11,15,53] however, this is not consistent with cluster based descriptions of the magnetic ordering behavior. The hydrogen effects are reversible in the sense that driving the hydrogen out of the samples by annealing in vacuum restores the original magnetic behavior. Thus no permanent structural or chemical changes are associated with the hydrogen-induced changes to the magnetic ordering—if distinguishable clusters are present before the hydrogen is added and after it has been removed, then they must also be present in the hydrided state, but no longer able to reduce T_c or cause noncollinearity when they order.

There is no way for hydrogen to affect the γ-Fe clusters proposed in the FM-AF model. First, they are chemically distinct so they cannot disappear when hydrogen is introduced into the matrix, and second, as hydrogen has no affinity for iron and the dense-packed fcc form has no voids large enough to accommodate a hydrogen atom, no hydrogen will enter the AF clusters. If they were the origin of noncollinearity in the original alloy then they must also cause the hydride to be noncollinear, unless for some reason they are completely decoupled from the hydride matrix, in which case they would contribute a substantial (20–30 %) paramagnetic component to the spectra above 70 K (T_N for the γ-Fe clusters). This component is never observed.

While both the FM matrix and the FM clusters may be expected to absorb hydrogen as they are supposed to be chemically similar, it is not clear that this should affect the cluster-matrix isolation required by the FM-FM model to cause the noncollinearity. Both the fluctuations in interatomic spacing and the stresses due to the cluster-matrix mismatch must still be present in the hydride, and as these form the basis for the FM-matrix plus isolated FM-cluster model, the predicted magnetic behavior should be largely unchanged. It is possible to imagine that the expansion could allow ferromagnetic coupling to develop between the clusters and matrix, but this must be a reversible process and demands that the influence of the clusters depends on a very delicate balance between competing effects. This balance, and relatively easy suppression of the clusters, implies that the magnetic properties

are extremely sensitive to internal stresses and they should therefore also be strongly affected by preparation conditions, a requirement that is not consistent with the reproducibility clear in Fig. 10.

In conclusion, both of the cluster models are unable to account for the observed magnetic phase diagram of *a*-Fe-Zr; they predict a loss of ferromagnetic order at low temperatures in direct contradiction of the experimental evidence. Despite the profound influence the clusters are supposed to exert on the magnetic ordering, and the large volume fraction they supposedly occupy, there is no direct experimental evidence for their existence.

Homogeneous exchange frustration model

All of the changes seen in Fig. 7 can be explained in terms of homogeneous exchange frustration, arising through the distance dependence of the direct Fe-Fe exchange interaction. Furthermore, the behavior of *a*-$Fe_{91}Sc_9$ is fully consistent with this model.

Earlier work has shown that T_c actually starts to drop when the Fe content exceeds ~ 85 at. %, while the average iron moment continues to increase slightly.[54] T_c is determined by the product of the average moment and the average exchange strength, with large moments coupled by strong exchange leading to a high T_c. Since the average iron moment does not decrease when the Fe concentration is raised from 85 to 93 at. %, the decrease of T_c must be due to a decrease in the average exchange strength. Monte Carlo simulations of a Heisenberg spin system with exchange frustration[3,28] indicate that as soon as antiferromagnetic interactions are present, two magnetic transitions are observed. Since there is no evidence of a second transition in alloys with Fe concentrations below 89 at. %, we conclude that the exchange interactions in these alloys remain ferromagnetic, and that the decrease of T_c in this range is due mainly to a reduction in the FM interaction strength. For alloys showing two magnetic transitions ($x \geq 90$), the drop of T_c and therefore the reduction of exchange strength includes a contribution from the presence of AF interactions.

Anomalous x-ray scattering indicates that the Fe-Fe separation in *a*-Fe_xZr_{100-x} alloys with x around 90% is about 2.6 Å,[55,56] which is close to the critical separation of 2.55 Å where the exchange interaction changes sign from FM to AF. The wide distribution of Fe-Fe separations in these amorphous alloys, coupled with the strong distance dependence of the exchange interactions in the region of the typical interatomic spacing, will lead to a wide distribution of exchange interactions which may include both FM and AF components. When the iron concentration is increased in *a*-Fe-*T* alloys, the average Fe-Fe separation becomes smaller since the radius of the Fe atoms is less than that of any of the alloying elements (Zr, Hf, and Sc); consequently the strengths of the FM interactions are first reduced and then contacts short enough for AF interactions appear. This strong sensitivity of the magnetic behavior to the Fe-Fe separation can be checked at fixed iron concentration in two ways: (i) hydrostatic pressure reduces the interatomic separation and drives T_c down in both *a*-Fe-Zr (Ref. 57) and *a*-Fe-Hf (Ref. 21) at a rate of ~ 7 K/kBar and (ii) adding hydrogen increases the interatomic separation and leads to a substantial increase in T_c in all of these systems.[10,58–61] It is important to note that adding hydrogen also eliminates the noncollinearity associated with exchange frustration.[10,11]

We therefore conclude that the reduction of T_c with increasing Fe content must be largely due to the decrease of the nearest-neighbor Fe-Fe separations, which first reduces the average strength of the FM interactions and then leads to the presence of AF interactions.

Once the presence of AF exchange interactions is accepted, the magnetic behavior shown in Fig. 7 follows naturally. Both Ising[1,62] and Heisenberg[2] mean-field models for partially frustrated systems yield phase diagrams identical to that shown above in Fig. 7. Increasing frustration is predicted to lead to a drop in T_c and the appearance of a second transition, T_{xy}, which rises to join T_c. These models are homogeneous, in that below T_{xy} any spin can be more or less strongly canted from the mean direction, and we cannot distinguish regions of FM and SG spins. Above T_{xy} and below T_c, all of the spins are ferromagnetically aligned, rather than there being clusters of "melted spin-glass" spins and a residual ferromagnetic matrix. Both models predict that T_c remains a ferromagnetic phase transition and this is consistent with our experimental observations. Our modified Arrott plots yield both straight critical isotherms, and transition temperatures fully consistent with Mössbauer measurements despite the fact that the two measurements represent radically different time averages over the system dynamics. Below the second transition, the spin system becomes noncollinear through the ordering of transverse spin components. This ordering must be distinguished from "canting" which implies a change in the direction of **M** with $|M|$ constant, since in transverse spin freezing the direction of **M** changes through the ordering of xy components at constant M_z, and $|M|$ increases. This picture may be somewhat idealized, as the mean-field model predicts spin-glass ordering in the xy plane, whereas there is some evidence of correlations in these components.[63–65] Another key prediction of the mean-field model is that the ferromagnetic order established at T_c does not decay below T_{xy}. Both neutron depolarization[51] and Lorentz microscopy[49,50,66] confirm that long-range ferromagnetic order is established at T_c and not lost at or below T_{xy}, ruling out any model predicting a truly reentrant transition to a disordered state.

All of the experimental observations discussed in this work have been reproduced by Monte Carlo simulations[3,28] of classical Heisenberg spins placed on a simple cubic lattice with nearest-neighbor interactions. While these calculations are restricted to relatively small systems (16^3), they more closely match the experimental materials, which are expected to be dominated by nearest-neighbor exchange, rather than the ∞-ranged interactions assumed in mean-field models. Furthermore, they allow the system dynamics to be examined in detail and yield important insights into the ordering. Three-dimensional (3D) Heisenberg Monte Carlo simulations

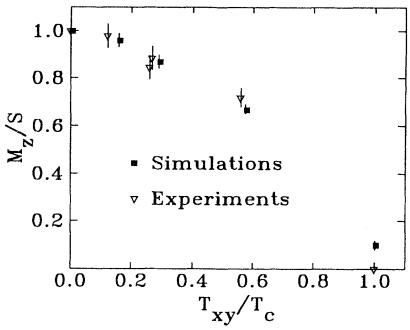

FIG. 11. Normalized comparison of our experimental transition temperatures and noncollinearity data with results of Monte Carlo simulations of the 3D Heisenberg model with random $\pm J$ exchange bonds.[3,28] Note excellent agreement.

have reproduced not only the phase diagram, but also the experimental signatures associated with homogeneous transverse spin freezing at T_{xy}.[3,4,28]

Exchange frustration was modeled by randomly replacing a fraction, f, of the FM interactions by AF bonds. The exchange distribution was assumed to have a two δ-function form ($+J$ and $-J$) for simplicity. Several parameters corresponding to experimentally accessible quantities were followed in both temperature and frustration, including the average spin length, $S_{\rm rms}$ (approximately equivalent to $\langle B_{\rm hf}\rangle$) and the magnetization **M**. The simulations predict that increasing the fraction of AF bonds (and thus the degree of frustration) causes T_c to fall, reflecting the decrease of the average exchange interaction, while T_{xy} rises due to the increase of frustration level. For a simple cubic lattice, T_c and T_{xy} meet at a critical fraction $f_c=0.25$. After that point, the system undergoes a single transition from paramagnet to spin glass with $T_{\rm sg}\simeq 0.42T_H$ (the ferromagnetic transition temperature for $f=0$).

In order to make quantitative comparisons between the simulations and our experiments, it is necessary to relate our alloy compositions, x, to the fraction of frustrated bonds, f, in the model calculations. As we have no direct way of measuring the exchange distribution, or indeed of mapping a real distribution onto the two δ-function form used in the simulations, we have chosen an alternative method. Taking the ratio of T_{xy} to T_c as a measure of degree of frustration, we can compare the degree of noncollinearity predicted by the model with that observed in our alloys by plotting $M/S_{\rm rms}$ (or $M_z/\mu_{\rm av}$ in the case of the experimental results) vs T_{xy}/T_c. The results are shown for all of the alloys studied here in Fig. 11, and the agreement between the simulations and measurements is remarkable. This agreement strongly supports the view that exchange frustration alone (the only mechanism in the simulations) is sufficient to account for the observed magnetic ordering behavior of the iron-rich amorphous binary alloys studied here.

V. CONCLUSIONS

The magnetic properties of iron-rich amorphous alloys in the form of Fe_xT_{100-x} (T=Zr, Hf, Sc; $89\le x\le 93$) have been studied systematically, mainly by Mössbauer spectroscopy and magnetization measurements. The presence of both ferromagnetic and antiferromagnetic exchange interactions in these alloys leads to exchange frustration and therefore complex magnetic ordering behavior, which can be understood in terms of a homogeneous transverse spin freezing model. Within this model, the alloys containing Zr and Hf are partially frustrated, exhibiting two magnetic transitions (T_c and T_{xy}), while a-$Fe_{91}Sc_9$ is fully frustrated: T_c has merged with T_{xy} to form a single transition to a random isotropically frozen state.

Alternative, inhomogeneous models have been shown to be inconsistent with several key experimental observations. Furthermore, there is no direct evidence to support the suggestion that magnetically distinct, isolated clusters are present in these alloys.

All of our experimental observations have been reproduced by Monte Carlo simulations, where the only mechanism included is exchange frustration modeled by randomly replacing a fraction of FM interactions with AF interactions. The quantitative agreement between our results and the simulations demonstrates that the magnetic ordering behavior of the alloys studied here is controlled primarily by exchange frustration.

ACKNOWLEDGMENTS

This work was supported by grants from the Natural Sciences and Engineering Research Council of Canada and Fonds pour la Formation de Chercheurs et l'aide à la Recherche, Québec. We are grateful to Dr. C. Stager at McMaster University, for assistance with the SQUID magnetometry.

[1]S. Kirkpatrick and D. Sherrington, Phys. Rev. B **17**, 4384 (1978).
[2]M. Gabay and G. Toulouse, Phys. Rev. Lett. **47**, 201 (1981).
[3]J. R. Thomson, Guo Hong, D. H. Ryan, M. J. Zuckermann, and M. Grant, Phys. Rev. B **45**, 3129 (1992).
[4]D. H. Ryan, in *Recent Progress in Random Magnets*, edited by D. H. Ryan (World Scientific, Singapore, 1992).
[5]K. Moorjani and J. M. D. Coey, *Magnetic Glasses* (Elsevier, Amsterdam, 1984).
[6]R. K. Day, J. B. Dunlop, C. P. Foley, M. Ghafari, and H. Pask, Solid State Commun. **56**, 843 (1985).
[7]D. H. Ryan, J. O. Ström-Olsen, W. B. Muir, J. M. Cadogan, and J. M. D. Coey, Phys. Rev. B **40**, 11 208 (1989).
[8]J. M. D. Coey, D. Givord, A. Liénard, and J. P. Rebouillat, J. Phys. F **11**, 2707 (1981).
[9]J. Chappert, J. M. D. Coey, A. Liénard, and J. P. Rebouillat, J. Phys. F **11**, 2727 (1981).
[10]D. H. Ryan, J. M. D. Coey, E. Batalla, Z. Altounian, and J. O. Ström-Olsen, Phys. Rev. B **35**, 8630 (1987).
[11]D. H. Ryan, J. M. D. Coey, and J. O. Ström-Olsen, J. Magn.

Magn. Mater. **67**, 148 (1987).
[12]P. A. Beck, Phys. Rev. B **32**, 7255 (1985).
[13]W. Kummerle and U. Gradmann, Solid State Commun. **24**, 33 (1977).
[14]G. J. Johanson, M. B. McGirr, and D. A. Wheeler, Phys. Rev. B **1**, 3208 (1970).
[15]H. Ma, Z. Wang, H. P. Kunkel, G. Williams, D. H. Ryan, and J. O. Ström-Olsen, J. Magn. Magn. Mater. **104-107**, 89 (1992).
[16]H. Hiroyoshi and K. Fukamichi, Phys. Lett. **84A**, 242 (1981).
[17]N. Saito, H. Hiroyoshi, K. Fukamichi, and Y. Nakagawa, J. Phys. F **16**, 911 (1986).
[18]D. H. Ryan, J. O. Ström-Olsen, R. Provencher, and M. Townsend, J. Appl. Phys. **64**, 5787 (1988).
[19]This sample was previously identified as being a-$Fe_{92}Zr_8$; however, the transition temperatures observed suggested that the actual iron content was 93 at. %. Subsequent microprobe analysis confirmed this revised composition.
[20]D. H. Ryan and Hong Ren, J. Appl. Phys. **69**, 5057 (1991).
[21]K. Fukamichi, K. Shirakawa, T. Kaneko, and T. Masumoto, *Rapidly Quenched Metals,* edited by S. Steeb and H. Warlimont (Elsevier Science, Amsterdam, 1985).
[22]H. Hiroyoshi, K. Noguchi, K. Fukamichi, and Y. Nakagawa, J. Phys. Soc. Jpn. **54**, 3554 (1985).
[23]S. H. Liou, G. Xiao, J. N. Taylor, and C. L. Chien, J. Appl. Phys. **57**, 3536 (1985).
[24]D. A. Read, T. Moyo, S. Jassim, R. A. Dunlap, and G. C. Hallam, J. Magn. Magn. Mater. **82**, 87 (1989).
[25]S. N. Kaul, V. Siruguri, and G. Chandra, Phys. Rev. B **45**, 12 343 (1992).
[26]B. Window, J. Phys. E **4**, 401 (1971).
[27]D. Kaptas and I. Vincze, Hyperfine Interact. **55**, 987 (1990).
[28]J. R. Thomson, Guo Hong, D. H. Ryan, M. J. Zuckermann, and M. Grant, J. Appl. Phys. **69**, 5231 (1991).
[29]S. Lange, M. M. Abd-Elmeguid, and H. Micklitz, Phys. Rev. B **41**, 6907 (1990).
[30]R. Reisser, M. Fähnle, and H. Kronmüller, J. Magn. Magn. Mater. **75**, 45 (1988).
[31]S. N. Kaul, J. Phys. F **18**, 2089 (1988).
[32]J. C. Le Guillou and J. Zinn-Justin, Phys. Rev. Lett. **39**, 95 (1977).
[33]The Sn^{119} was introduced for a study of transferred hyperfine fields at a nonmagnetic site (see Ref. 63). Comparison with a Sn-free sample showed that the two alloys had identical transition temperatures and magnetizations. Results from the Sn-doped sample are used here as they are more complete.
[34]J. M. D. Coey, J. Appl. Phys. **49**, 1646 (1978).
[35]J. R. Thomson, Ph.D. thesis, McGill University, 1992.
[36]M. Ghafari, R. K. Day, J. B. Dunlop, and A. C. McGrath, J. Magn. Magn. Mater. **104-107**, 1668 (1992).
[37]D. A. Read, T. Moyo, and G. C. Hallam, J. Magn. Magn. Mater. **44**, 279 (1984).
[38]U. Gonser, C. J. Meechan, A. H. Muir, and H. Wiedersich, J. Appl. Phys. **34**, 2373 (1963).
[39]Y. Tsunoda, S. Imada, and N. Kunitomi, J. Phys. F **18**, 1421 (1988).
[40]S. N. Kaul, J. Phys. Condens. Matter **3**, 4027 (1991).
[41]J. J. Rhyne, R. W. Erwin, J. A. Fernandez-Baca, and G. E. Fish, J. Appl. Phys. **63**, 4080 (1988).
[42]S. Brauer, Ph.D. thesis, McGill University, 1992.
[43]G. E. Fish and J. J. Rhyne, J. Appl. Phys. **61**, 454 (1987).
[44]D. Kaptas, T. Kemeny, J. Balogh, L. F. Kiss, L. Granasy, and I. Vincze, Hyperfine Interact. **94**, 1861 (1994).
[45]G. LeCaer, J. M. Dubois, H. Fischer, U. Gonser, and H. G. Wagner, Nucl. Instrum. Methods B **5**, 25 (1984).
[46]Y. Xu, W. B. Muir, and Z. Altounian (unpublished).
[47]R. Brüning and J. O. Ström-Olsen, Phys. Rev. B **41**, 2678 (1990).
[48]J. O. Ström-Olsen, D. H. Ryan, and Z. Altounian, Mater. Sci. Eng. A **133**, 403 (1991).
[49]S. Senoussi, S. Hadjoudj, R. Fourmeaux, and C. Jaouen, J. Phys. (Paris) Colloq. **49**, C8-1163 (1988).
[50]S. Hadjoudj, S. Senoussi, and D. H. Ryan, J. Appl. Phys. **67**, 5958 (1990).
[51]S. Hadjoudj, S. Senoussi, and I. Mirebeau, J. Magn. Magn. Mater. **93**, 136 (1991).
[52]Hong Ren and D. H. Ryan, J. Appl. Phys. **73**, 5494 (1993).
[53]J. M. D. Coey, A. Liénard, J. P. Rebouillat, D. H. Ryan, Yu Boliang, and Wang Zhenxi, J. Phys. F **18**, 1299 (1988).
[54]K. M. Unruh and C. L. Chien, Phys. Rev. B **30**, 4968 (1984).
[55]H. U. Krebs, W. Biegel, A. Bienenstock, D. J. Webb, and T. H. Geballe, Mater. Sci. Eng. **97**, 163 (1988).
[56]M. Przbylski, K. Krop, T. Stobiecki, and L. Dargel-Sulir, Hyperfine Interact. **27**, 425 (1986).
[57]T. Kaneko, K. Shirakawa, S. Ohnuma, M. Nose, H. Fujimori, and T. Masumoto, J. Appl. Phys. **2**, 1826 (1981).
[58]J. Tanaka, K. Nomura, Y. Ujihira, A. Vértes, H. Kimura, and T. Masomoto, Hyperfine Interact. **55**, 1071 (1990).
[59]A. H. Morrish, R. J. Pollard, Z. S. Wronski, and A. Calka, Phys. Rev. B **32**, 7528 (1985).
[60]S. M. Fries, C. L. Chien, J. Crummenauer, H. G. Wagner, and U. Gonser, J. Less-Common Met. **130**, 17 (1987).
[61]E. Kuzmann, A. Vértes, Y. Ujihira, P. Kovács, T. Ando, and T. Masomoto, Hyperfine Interact. **45**, 279 (1989).
[62]D. Sherrington and S. Kirkpatrick, Phys. Rev. Lett. **25**, 1792 (1975).
[63]Hong Ren and D. H. Ryan, Phys. Rev. B **47**, 7919 (1993).
[64]M. M. Abd-Elmeguid, H. Micklitz, R. A. Brand, and W. Keune, Phys. Rev. B **33**, 7833 (1986).
[65]A. Ait-Bahammou, C. Meyer, F. Hartmann-Boutron, Y. Gros, and I. A. Campbell, J. Phys. (Paris) Colloq. **49**, C8-1157 (1988).
[66]S. Senoussi, S. Hadjoudj, P. Jouret, J. Bilotte, and R. Fourmeaux, J. Appl. Phys. **63**, 4086 (1988).
[67]H. Tange, Y. Tanaka, M. Goto, and J. Fukamichi, J. Magn. Magn. Mater. **81**, L243 (1989).
[68]H. Ma, H. P. Kunkel, and G. Williams, J. Phys. Condens. Matter **3**, 5563 (1991).